

## Thermionic Converters Operating in the Ignited Mode. Part II: A Quasi-Equilibrium Model for the Interelectrode Plasma\*

DANIEL R. WILKINS AND ELIAS P. GYFTOPOULOS

*Department of Nuclear Engineering and Research Laboratory of Electronics,  
Massachusetts Institute of Technology, Cambridge, Massachusetts*

(Received 6 December 1965; in final form 2 February 1966)

A multistage ionization-recombination model is proposed to describe the formation and loss of atomic ions in low-energy cesium plasmas. Solutions of the ambipolar diffusion equation are investigated with due consideration given to these processes. The solutions indicate the existence of a state of quasi-equilibrium throughout most of a low-energy plasma in which the electron temperature is more than several hundred degrees above a critical ignition temperature.

The assumption of quasi-equilibrium in the interelectrode plasma of a thermionic converter operating in the collisional ignited mode is shown to result in a plasma model which correlates a wide variety of experimental data. Included in the successful correlations are electron random current density and temperature profiles as well as output-current characteristics.

The experimentally observed state of quasi-equilibrium in thermionic converter plasmas is found to be near the Saha-equilibrium limit. It is therefore concluded that the multistage ionization-recombination processes in these plasmas involve numerous excited states.

### 1. INTRODUCTION

THE purpose of this paper is to develop a plasma model suitable for the representation of the phenomena occurring in cesium thermionic converters operating in the collisional ignited mode.

Several conceptually different plasma models for cesium thermionic converters have been proposed. References 1 and 2 are two examples. These models predict output-current characteristics which are in good agreement with experimental data. It is shown in Part I,<sup>3</sup> however, that successful correlation of output-current characteristics is necessary but not sufficient to verify the validity of a particular plasma model. Consequently, a primary objective of this analysis is to develop a model which leads to results in good agreement both with measured output-current characteristics and with measured plasma electron density and temperature profiles in the interelectrode space.

The paper is organized as follows. In Sec. 2, the plasma-transport equations are solved by assuming that the plasma in the interelectrode space is in a state of quasi-equilibrium. It is shown that this state is a consequence of the ambipolar diffusion equation for a variety of ionization and recombination mechanisms. In Sec. 3, output-current characteristics are derived according to the formalism of Part I.<sup>3</sup> In Sec. 4, the electron density and temperature profiles and the output-current characteristics derived in Secs. 2 and 3 are compared with existing experimental data. Agreement between theoretical and experimental results is

established. The major conclusions of the analysis are summarized in Sec. 5.

The nomenclature of Part I<sup>3</sup> is applicable. Only symbols not appearing in Part I are defined herein.

### 2. PLASMA ANALYSIS

#### 2.1. Plasma Transport Equations

A set of transport equations for plasmas in the interelectrode space of cesium thermionic converters is derived elsewhere.<sup>4</sup> This is the set of Eqs. (1) in Ref. 3, and it is not repeated. Only the source term  $S$  and the energy transfer term  $Q_e$  are derived for a multistage ionization process.

#### 2.2. Source and Energy Transfer Terms

It is assumed that atomic ions are formed from excited states of cesium through a general multistage ionization process, and destroyed through the inverse of the ionization process, i.e., through three-body recombination.<sup>5</sup> Thus, the net rate of charged-particle production per unit volume at position  $x$  of the plasma is given by the relation

$$S(x) = \sum_{s=0} [R_{is}(x) - R_{rs}(x)], \quad (1)$$

where  $R_{is}(x)$  and  $R_{rs}(x)$  are the rates of ionization from and recombination into excited state  $s$ , respectively. The subscript "s" is a running index for excited state  $s$  and does not necessarily correspond to any of the quantum numbers associated with the state. The ground state is denoted by  $s=0$ .

The rate of ionization from excited state  $s$  is given by

<sup>4</sup> D. R. Wilkins and E. P. Gyftopoulos, J. Appl. Phys. (to be published).

\* This work was supported principally by the National Science Foundation (Grant GK-614).

<sup>1</sup> N. S. Rasor, "Analytical Description of Cesium Diode Phenomenology," 25th Annual Conference on Physical Electronics, MIT, Cambridge, Mass., March 1965.

<sup>2</sup> H. L. Witting and E. P. Gyftopoulos, J. Appl. Phys. **36**, 1328 (1965).

<sup>3</sup> D. R. Wilkins and E. P. Gyftopoulos, J. Appl. Phys. **37**, 2888 (1966) (preceding paper).

the relation

$$R_{is}(x) = N_s \int f_e(x, \bar{v}_e) v_e \sigma_{is}(v_e) d^3 v_e, \quad (2)$$

where  $N_s$  is the density;  $\sigma_{is}(v_e)$  is the ionization cross section of excited state  $s$ ;  $f_e(x, \bar{v}_e)$  is the electron distribution function; and  $v_e$  is the electron speed. For near-Maxwellian distributions of the form derived in Ref. 4, Eq. (2) reduces to

$$R_{is}(x) = N_s n_e \bar{v}_e \hat{\sigma}_{is}(T_e) \exp[-eV_{is}/kT_e], \quad (3)$$

where  $\bar{v}_e$  is the average electron speed,  $V_{is}$  is the ionization potential, and  $\hat{\sigma}_{is}(T_e)$  is an effective ionization cross section defined by the relation

$$\hat{\sigma}_{is}(T_e) = \int_0^\infty \left( Z + \frac{eV_{is}}{kT_e} \right) \sigma_{is}(v_e) \exp(-Z) dZ$$

for  $Z = \frac{m_e v_e^2}{2kT_e} - \frac{eV_{is}}{kT_e}$ .

If the excited state  $s$  is in thermodynamic equilibrium with the free electrons, then

$$n_e^2 = (\omega_0/\omega_s) (2\pi m_e kT_e/h^2)^3 N_s \exp(-eV_{is}/kT_e), \quad (4)$$

where  $\omega_s$  is the statistical weight. Combination of Eqs. (3) and (4) and use of the principle of detailed balance<sup>5</sup> yields that the rate of three-body recombination into excited state  $s$  is given by the relation

$$R_{rs}(x) = (\omega_s/\omega_0) (2\pi m_e kT_e/h^2)^{-3/2} \bar{v}_e \hat{\sigma}_{is}(T_e) n_e^3. \quad (5)$$

It follows from Eqs. (1), (3), and (5) that

$$S(x) = \nu_i n_e - \beta_r n_e^3, \quad (6)$$

$$\nu_i = N_0 \bar{v}_e \hat{\sigma}_{i0}(T_e) \exp(-eV_{i0}/kT_e) \times [1 + \sum_{s>0} \psi_s \omega_s \hat{\sigma}_{is}(T_e) / \omega_0 \hat{\sigma}_{i0}(T_e)],$$

$$\beta_r = (2\pi m_e kT_e/h^2)^{-3/2} \bar{v}_e \sum_{s=0} \omega_s \hat{\sigma}_{is}(T_e) / \omega_0.$$

The factor  $\psi_s$  is the ratio of the density of state  $s$  to that which would exist if the plasma were in local thermodynamic equilibrium at the same neutral particle density and electron temperature. In other words:

$$\psi_s = (\omega_0/\omega_s) (N_s/N_0) \exp[e(V_{i0} - V_{is})/kT_e].$$

Note that although the form of Eq. (6) is valid for general multistage ionization and recombination processes, the quantities  $\nu_i$  and  $\beta_r$  depend strongly upon which excited states participate in these processes. Values of  $\nu_i$  and  $\beta_r$  for specific mechanisms are given by others.<sup>1,5</sup> For the purposes of this study, however,  $\nu_i$  and  $\beta_r$  are left as unspecified functions of the electron temperature only. This is equivalent to assuming that the ratios  $\psi_s$  are insensitive to plasma variables other than  $T_e$ .

<sup>5</sup> E. Hinnov and J. G. Hirschberg, Phys. Rev. 125, 795 (1962).

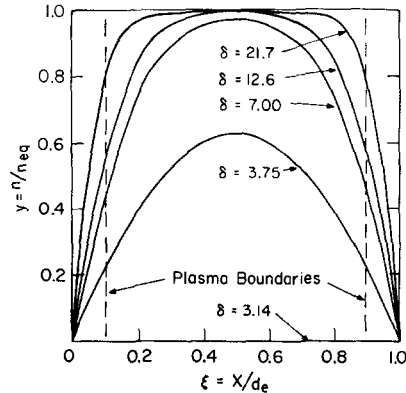


FIG. 1. Solutions of ambipolar diffusion equation for uniform  $T_e$ .

The electron kinetic energy transfer term  $Q_e$  is given by the relation

$$Q_e(x) = eV_{i0} S(x) = V_{i0} dJ_i/dx = V_{i0} dJ_e/dx, \quad (7)$$

if it is assumed that energy transfer is primarily associated with the ionization and recombination processes. In other words,  $Q_e$  is given by Eq. (7) if it is assumed that radiation losses, from all excited states to the electrodes of the plasma, are negligible.

### 2.3. Ambipolar Diffusion Equation

The ion and electron current differential equations [Eqs. (1a), (1c), and (1d) in Ref. 3] can be reduced to an ambipolar diffusion equation by assuming that  $n_e \approx n_i$ . Thus, to a good approximation, it is found that

$$-\frac{d}{dx} \left( D_a \frac{dn_e}{dx} \right) = \nu_i n_e - \beta_r n_e^3, \quad (8)$$

where the ambipolar diffusion coefficient

$$D_a = \mu_i k(T_i + T_e)/e.$$

Although, in general, the electron temperature and hence the parameters  $D_a$ ,  $\nu_i$ , and  $\beta_r$  are not constant, it is of interest to consider the solutions of Eq. (8) for the special case of a uniform electron temperature. To this end, when  $T_e$  is independent of  $x$ , Eq. (8) may be written in the dimensionless form

$$\frac{d^2 y}{d\xi^2} = -\delta^2 y(1-y^2), \quad y = \frac{n_e}{n_{eq}}, \quad n_{eq}^2 = \frac{\nu_i}{\beta_r}, \quad \xi = \frac{x}{d_e}, \quad \delta^2 = \frac{\nu_i d_e^2}{D_a}, \quad (9)$$

where  $d_e$  is the effective plasma thickness including extrapolation lengths, and  $n_{eq}$  is the quasi-equilibrium solution in the absence of diffusion. The solutions of Eq. (9) are Jacobi elliptic functions.<sup>6</sup> Subject to the boundary conditions that  $y=0$  at the extrapolated

<sup>6</sup> H. T. Davis, Introduction to Nonlinear Differential and Integral Equations (Dover Publications Inc., New York, 1962)

boundaries, these solutions are shown in Fig. 1. Several important features of the solutions are evident from the figure:

(a) For  $\delta < \pi$  the only solution is  $y=0$ . Physically this implies that insufficient ions are produced by volume ionization to sustain a plasma.

(b) The condition  $\delta = \pi$  may be interpreted as an ignition criterion which defines the minimum electron temperature, the ignition temperature, necessary to establish a self-sustained plasma.

(c) For  $\delta > \pi$  nontrivial solutions exist. Note that an increase of  $\delta$  by less than an order of magnitude above  $\pi$  leads to solutions which are  $y \approx 1$  ( $n \approx n_{eq}$ ) virtually throughout the entire thickness of the plasma. Since  $\delta$  depends exponentially on  $T_e$ , the transition from the diffusion-dominated solution ( $y \approx 0$ ) to the ionization-recombination-dominated solution ( $y \approx 1$ ) is stimulated by a very slight increase, of the order of a few hundred degrees, of the electron temperature above the ignition temperature.

(d) The values of the ignition temperature and  $n_{eq}$  depend on the cesium pressure, the plasma thickness, and the ionization-recombination mechanisms. However, the existence of the ignition temperature and the rapid transition to  $n_{eq}$  as the electron temperature is increased are properties of Eq. (9) for all multi-stage ionization-recombination mechanisms. The importance of this conclusion is that serious errors may be introduced if recombination is neglected. For example, the "catastrophe" which appears in many thermionic converter plasma analyses, if a critical pressure-spacing product is exceeded,<sup>7,8</sup> can be directly attributed to the omission of recombination. Similar results are derived for boundary conditions which account for surface ionization.

#### 2.4. Quasi-Equilibrium Plasma Hypothesis

The analysis for uniform  $T_e$  may be extended to cesium plasmas with nonuniform electron temperature. Quasi-equilibrium would then mean that most of the plasma is ionization-recombination dominated and that there is a local relation between electron density and temperature at each point in the plasma. This relation is

$$n_e^2 = n_{eq}^2 = \nu_i / \beta_r = \psi_e^2(T_e) (2\pi m_e k T_e / \hbar^2)^{3/2} N_0 \times \exp[-eV_{i0} / kT_e], \quad (10)$$

$$\psi_e^2(T_e) = \left[ 1 + \sum_{s>0} \frac{\omega_s}{\omega_0} \frac{\hat{\sigma}_{is}(T_e)}{\hat{\sigma}_{i0}(T_e)} \right] / \left[ 1 + \sum_{s>0} \frac{\omega_s}{\omega_0} \frac{\hat{\sigma}_{is}(T_e)}{\hat{\sigma}_{i0}(T_e)} \right].$$

<sup>7</sup> N. S. Rasor and S. Kitrilakis, "Basic and Engineering Implications of Correlated Converter Phenomenology," Thermionic Conversion Specialist Conference, Cleveland, Ohio, October 1964.

<sup>8</sup> S. Kitrilakis, A. Shavit, and N. Rasor, "The Departure of Observed Performance from the Idealized Case in Cesium Thermionic Converters," 24th Annual Conference on Physical Electronics, MIT, Cambridge, Mass., March 1964.

If the plasma is in local thermodynamic equilibrium with the temperature  $T_e(x)$ , i.e.,  $\psi_e = 1$ , then Eq. (10) is identical with the Saha equation and  $\psi_e(T_e) = 1$ . If some excited states are depleted because, say, of radiative decay, then  $\psi_e(T_e) < 1$  and the quasi-equilibrium density is smaller than that given by the Saha equation.

It is postulated that Eq. (10) is valid for cesium plasmas existing in the interelectrode space of thermionic converters operating in the ignited mode. The factor  $\psi_e(T_e)$  is left unspecified but it is recognized as a weak function of  $T_e$ .

An equation similar in form to Eq. (10) is derived in Ref. 2 for a two-step molecular-ion production mechanism. Specifically:

$$n_e = 3.45 \times 10^{-4} N_0^2 T_a^{-1/2} \exp[-E_s / kT_e], \quad (11)$$

where  $E_s$  is the excitation energy of the 6P state of cesium and  $T_a$  (°K) is the background gas temperature. Consequently, Eq. (10) is formally valid for molecular as well as multistage atomic-ion formation processes.

#### 2.5. Solution of the Plasma Transport Equations

Equation (10) provides the basis for an approximate solution of the plasma transport equations with reference to a thermionic converter. To this end, differentiation of Eq. (10) yields

$$\frac{d(\ln n_e)}{d(\ln T_e)} = \left[ \frac{d(\ln \psi_e)}{d(\ln T_e)} + \frac{3}{4} + \frac{eV_{i0}}{2kT_e} \right] \gg 1. \quad (12)$$

Also, since  $J_i / J_e \approx \mu_i / \mu_e \ll 1$ , the output-current density  $J = \text{constant} = J_e - J_i \approx J_e$  and, after some algebra, the transport equations yield

$$E \approx - \frac{d}{dx} \left[ \left( \frac{5}{2} + k_e T \right) \frac{kT_e}{e} - \frac{1}{J} \left( \kappa_e \frac{dT_e}{dx} \right) \right]. \quad (13)$$

The meaning of Eqs. (12) and (13) is that fractional changes in the electron temperature and the electrical potential of the plasma are much smaller than those in electron density. Thus, neglect of the potential and temperature gradients in Eq. (1c) of Ref. 3 results in the relation

$$dJ_r / d\zeta + C_1 J_r + R_e J = 0; \quad \zeta = x/d; \quad C_1 = eJ \rho_e \infty d / kT_e; \quad R_e = e \hat{\sigma} d / 4 \mu_e \infty kT_e. \quad (14)$$

It is consistent with this approximation to write  $T_e \approx T_{e0} \approx T_{ed}$  is solving Eq. (14). Note that  $C_1$  is a measure of the resistive losses due to Coulomb collisions, and  $R_e$  is a measure of the interelectrode spacing measured in electron-neutral mean free paths. If the electron-neutral elastic collisions are treated as hard-sphere collisions,  $R_e = (\frac{3}{4}) N_0 \sigma_{en} d$ , where  $\sigma_{en}$  is the electron-neutral hard-sphere effective cross section.

The only boundary conditions necessary for the solution of Eq. (14) are those at the collector sheath. For a sheath of the type postulated in Part I<sup>3</sup> the electron

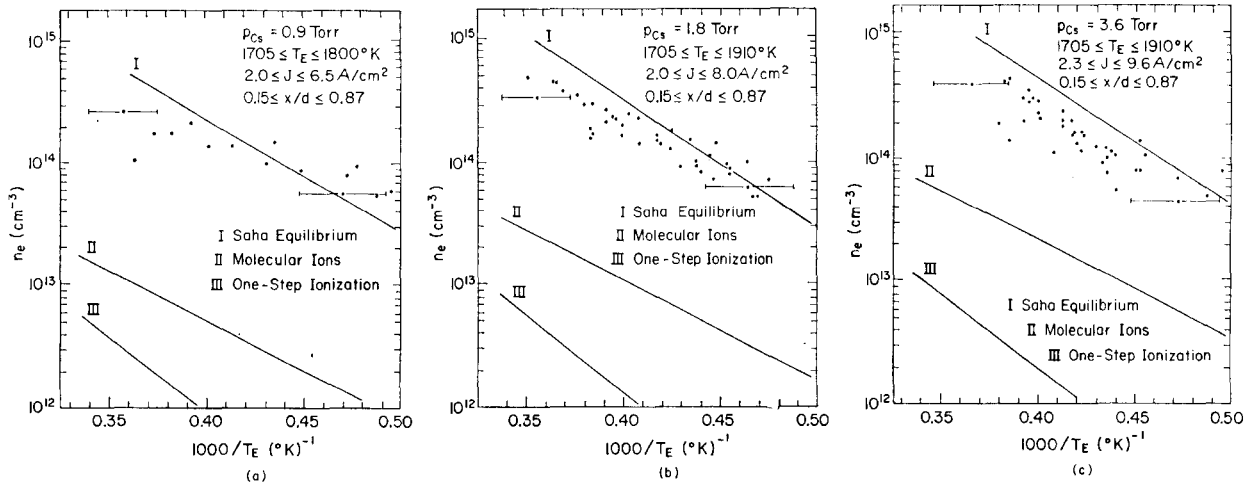


FIG. 2. Comparison of experimental<sup>9</sup> and theoretical electron density versus inverse electron temperature plots for (a)  $p_{Cs}=0.9$  Torr; (b)  $p_{Cs}=1.8$  Torr; (c)  $p_{Cs}=3.6$  Torr.

current and energy balances across the sheath yield

$$V_{CS} = \left(\frac{1}{2} + k_{ed}T\right) \frac{kT_{ed}}{e} \quad \text{and} \quad J_{rd} = J \exp\left(\frac{1}{2} + k_{ed}T\right). \quad (15)$$

Thus, the solution of Eq. (14) is given by the relation

$$\frac{J_r}{J} = \left(C_2 + \frac{R_e}{C_1}\right) \exp\left[C_1\left(1 - \frac{x}{d}\right)\right] - \frac{R_e}{C_1}; \quad (16)$$

$$C_2 = \exp\left[\frac{1}{2} + k_{ed}T\right].$$

If Coulomb resistive losses are negligible, i.e.,  $C_1 \ll 1$ , Eq. (16) reduces to the simple linear form

$$J_r/J \simeq C_2 + R_e \left(1 - \frac{x}{d}\right). \quad (16a)$$

Equations (10) and (16) or (16a) give the electron density and temperature profiles across the plasma.

The emitter sheath potential  $V_{ES}$  is found from the current balance across the emitter sheath. Thus,

$$V_{ES} = (kT_{e0}/e) \ln[J_{r0}/(J_E - J)]. \quad (17)$$

A conservative estimate for the emitter sheath polarity, to be as assumed in Part I<sup>3</sup>, is given by the relation

$$J/J_E \geq 1/(1 + C_2 + R_e). \quad (18)$$

Since usually  $C_2 > 2$  (see Sec. 4) and  $R_e$  is much greater than unity for the present collisional analysis to be applicable, Ineq. (18) is satisfied over a broad range of output current densities.

Two points regarding the implications and validity of the preceding analysis deserve special emphasis. First, Eqs. (14) through (18) are only implicitly dependent upon the quasi-equilibrium plasma assumption. They do not contain explicitly any parameters relating to the volume ionization and recombination processes. Thus, the electron density profiles do not yield information

concerning these processes. Such information may be obtained from measurements of the state of quasi-equilibrium itself (see Sec. 4). Second, the analysis may, fail near the plasma boundaries. Both the quasi-equilibrium plasma assumption and the approximations introduced in obtaining Eq. (14) are of questionable validity in the vicinity of the boundaries.

### 3. OUTPUT-CURRENT CHARACTERISTICS

If small electron temperature gradients in the plasma are neglected, i.e.,  $V_T \approx 0$ , and the random current density profiles are as computed in Sec. 2, Eq. (12) of Part I<sup>3</sup> for the output-current characteristics becomes

$$\frac{J_E}{J} = 1 + \left[ \left(1 + \frac{R_e}{C_1 C_2}\right) \exp C_1 - \frac{R_e}{C_1 C_2} \right] \times \left[ \frac{(J_E - J)}{J_1} \right]^{(V_0 - V)/(V_0 - V + 0.5V_{i0})} \quad (19)$$

$$J_1 \equiv \psi_e(T_{e0}) (2\pi m_e k T_{e0} / h^2)^{3/4} e \bar{v}_e N_0^{1/2} / 4C_2.$$

Note that  $J_1$  is a weak function of  $T_{e0}$ .

An excellent approximation to Eq. (19) is given by the relation

$$\frac{J_E}{J} = 1 + \left[ \left(1 + \frac{R_e}{C_1 C_2}\right) \exp C_1 - \frac{R_e}{C_1 C_2} \right] \times \left( \frac{J_E}{J_1} \right)^{(V_0 - V)/(V_0 - V + 0.5V_{i0})} \quad (19a)$$

Indeed, both for  $V \ll V_0$ , i.e.,  $J \approx J_E$ , and  $V = V_0$  Eqs. (19) and (19a) are identical while in the intermediate voltage range the maximum over-estimation in  $J$  given by Eq. (19a) is less than about 10% that given by Eq. (19). A further simplification of Eq. (19) obtains when Coulomb resistive losses are small ( $C_1 \ll 1$ ).

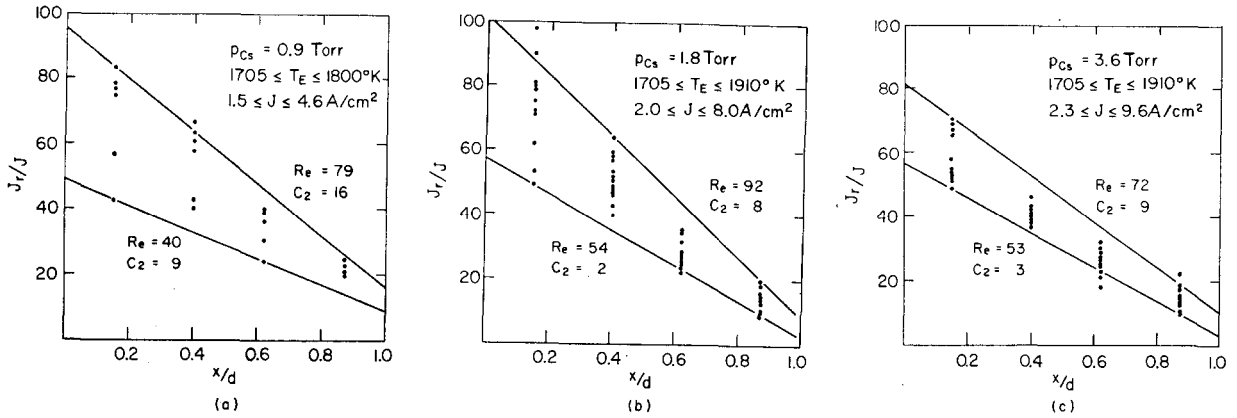


FIG. 3. Experimental<sup>9</sup> random current density profiles for (a)  $p_{Cs}=0.9$  Torr; (b)  $p_{Cs}=1.8$  Torr; (c)  $p_{Cs}=3.6$  Torr.

Specifically,

$$\frac{1}{J} \approx \frac{1}{J_E} + \frac{1}{J_E} \left(1 + \frac{d}{D}\right) \left(\frac{J_E}{J_1}\right)^{(V_0-V)/(V_0-V+0.5V_{i0})}, \quad (19b)$$

where  $D=C_2d/R_e$ .

When Eq. (19b) is applicable and the input parameters  $J_E$ ,  $D$ ,  $V_0$ , and  $J_1$  are known, this equation may be used to predict output-current characteristics. It is readily concluded that the characteristics are primarily sensitive to errors in  $J_E$ ,  $D$ , and  $V_0$  but not very sensitive to errors in  $J_1$ . The reason is that

$$\frac{\Delta J}{J} = [1-A(1-B)] \frac{\Delta J_E}{J_E} + (1-B) \left[ \frac{d}{d+D} \frac{\Delta D}{D} + A \frac{\Delta J_1}{J_1} + 2(1-A)^2 \ln(J_1/J_E) \frac{\Delta V_0}{V_{i0}} \right], \quad (20)$$

where  $A=(V_0-V)/(V_0-V+0.5V_{i0})$ ,  $B=J/J_E$ , and in the region of useful output power operation  $A \ll 1$  and  $B < 1$ .

On the other hand, if Eq. (19b) is applicable and an estimate of  $J_1$  is computed, but the remaining input parameters are not known, this equation provides a systematic procedure for the determination of the parameters from experimental data. Specifically, plots of  $1/J$  vs  $d$  for fixed cesium pressure  $p_{Cs}$  and various fixed output voltages, established from a variable spacing thermionic converter, should yield straight lines with a common intercept at the point  $d=-D$  and  $1/J=1/J_E$ . Thus,  $J_E$  and  $D$  can be determined and the emitter work function  $\phi_E$  and  $\sigma_{en}/C_2$  follow. In addition, if the slope of the  $1/J$  vs  $d$  lines is denoted by  $m$ , then,

$$z = -\ln(mJ_E D) / \ln(mJ_1 D) = 2(V_0 - V) / V_{i0}. \quad (21)$$

A plot of  $z$  vs  $2V/V_{i0}$  should yield a straight line with a slope equal to minus unity. The intercept of this line at  $z=0$  yields the contact potential  $V_0$  and, hence, the collector work function  $\phi_C$ .

Unfortunately, the above procedure is difficult to implement accurately in practice. The reason is that the  $1/J$  vs  $d$  plots (see Sec. 4) provide good estimates of  $J_E$  and  $m$ , with 10% error, but very poor estimates of  $D$ , with an error which may be up to several hundred per cent. Such poor estimates of  $D$  do not only result in poor estimates  $\sigma_{en}/C_2$ , but also in an impractical estimate of  $V_0$  [see Eq. (21)]. To avoid this difficulty, it is recommended that only two out of the three unknown parameters be derived from experimental plots of this type. For example, if  $D$  is independently and accurately known then Eq. (21) can be used to determine  $V_0$ . On the other hand, if  $\phi_C$  is independently known, it is convenient to rewrite Eq. (21) in the form

$$mJ_E = (1/D)(J_E/J_1)^{(V_0-V)/(V_0-V+0.5V_{i0})}. \quad (21a)$$

The meaning of Eq. (21a) is that given  $mJ_E$  and  $\phi_E$  from the  $1/J$  vs  $d$  plots and given  $\phi_C$ , then a plot of  $mJ_E$  vs  $(J_E/J_1)^{(V_0-V)/(V_0-V+0.5V_{i0})}$  should be a straight line with a slope equal to  $1/D$ . Such a plot yields an accurate value of  $D$ .

#### 4. COMPARISONS WITH EXPERIMENTAL DATA

##### 4.1. Validity of the Quasi-Equilibrium Plasma Hypothesis

Simultaneous spectroscopic measurements of the electron density and temperature profiles in thermionic converters under collision-dominated operating conditions have been reported by Reichelt.<sup>9</sup> The data are shown in Fig. 2 for three different cesium pressures. Also shown in Fig. 2 are three theoretical curves corresponding to Saha equilibrium [Eq. (10) with  $\psi_e(T_e)=1$ ], to molecular ion equilibrium [Eq. (11)], and to the equilibrium relation for a single-step ioniza-

<sup>9</sup> W. H. Reichelt, "Spectroscopic Investigation of the Ignited Mode of Thermionic Converter Operation," International Conference on Thermionic Electric Power Generation, London, England, September 1965.

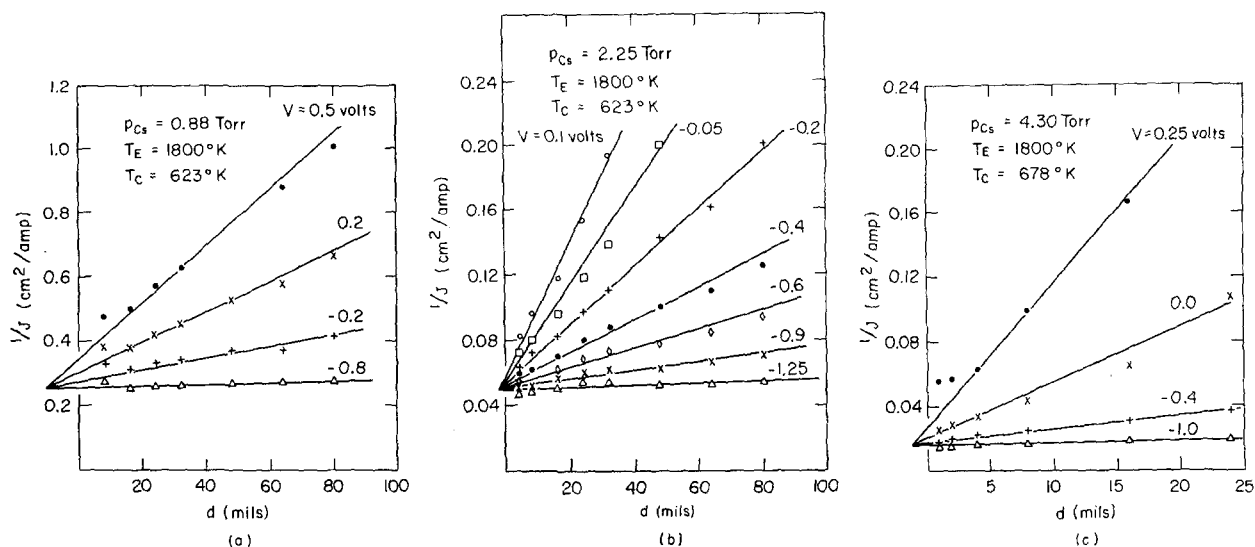


FIG. 4. Experimental results<sup>1</sup> on  $1/J$  vs  $d$  used for the determination of  $1/J_E$ :  
 (a)  $p_{Cs}=0.88$  Torr; (b)  $p_{Cs}=2.25$  Torr; (c)  $p_{Cs}=4.3$  Torr.

tion process based upon values of  $\nu_i$  and  $\beta_r$  given in Refs. 1 and 5, respectively.

Assuming Reichelt's measurements are accurate, several conclusions are forthcoming from Fig. 2. First, the data indicate that the interelectrode plasma is in a state of quasi-equilibrium. Second, this state is very close to complete Saha equilibrium at the local electron temperature, i.e.,  $\psi_e(T_e) \approx 1$ . Since recombination in cesium occurs most rapidly into the higher excited states,<sup>5</sup> this result implies that the higher excited states also participate in the ionization process. Thus, it may be inferred that the dominant ionization-recombination process is a multistage one, involving numerous excited states and leading to the formation of atomic cesium ions.

It should be emphasized that the preceding conclusions depend strongly on the accuracy of the measured electron temperatures. For example, a 15% increase in these temperatures would indicate a state of quasi-equilibrium considerably below the Saha limit for atomic ions.

#### 4.2. Electron Random Current Density Profiles

Experimental electron random current density profiles may be obtained from the measurements reported by Reichelt.<sup>9</sup> Typical results are shown in Fig. 3. The results are substantially scattered. Nevertheless, they indicate a linear relation between  $J_r/J$  and  $x/d$  and

TABLE I. Electron-neutral cross section and thermal diffusion ratio determined from Fig. 3.

Figure	$p_{Cs}$ (Torr)	$\sigma_{en}$ ( $\text{\AA}^2$ )	$k_{ed}^T$
3(a)	0.9	760-1500	1.7-2.3
3(b)	1.8	520-890	0.2-1.6
3(c)	3.6	260-360	0.6-1.7

suggest that Coulomb resistive losses are small so that Eq. (16a) is applicable. Thus, values of  $R_e$  and  $C_2$  may be determined from the slope and the intercept at  $x/d=1$  of straight lines drawn through the datum points. Because of the large scatter of the data, only two bounding lines for each cesium pressure are shown in Figs. 3(a) through (c). The corresponding values of  $R_e$  and  $C_2$  are also shown on each figure. Values of  $\sigma_{en}$  and  $C_2$  are given in Table I. In computing  $\sigma_{en}$  the background gas temperature is assumed equal to the linear average of the electrode temperatures.

The derived values of  $\sigma_{en}$  should be compared with those obtained from independent cross section or mobility measurements, i.e.,  $\sigma_{en} \approx 100-1000 \text{ \AA}^2$ , and the recommended value  $\sigma_{en} = 400 \text{ \AA}^2$ .<sup>10</sup> The reasons for the systematic variation in the values in Table I are not understood. Possible contributing factors are (a) the dependence of the electron mobility on the electron temperature; (b) collisional heating of the cesium gas; (c) inaccuracies in the experimental data. It should be pointed out that inclusion of Coulomb collision effects, i.e., use of Eq. (16) for the correlation of the random current density profiles, does not improve the agreement between theory and experiment.

The derived values of  $k_{ed}^T$  are realistic for typical elastic collision laws.<sup>4</sup> A theoretical estimate of  $k_{ed}^T$  is not attempted here. Suffice it to say that a range of values  $k_{ed}^T = 0.2-2.3$ , corresponding to  $C_2 = 2-16$ , is an acceptable result.

#### 4.3. Output-Current Characteristics

Figure 4 shows experimental  $1/J$  vs  $d$  plots for three sets of output-current characteristics reported in Ref. 1.

<sup>10</sup> J. M. Houston, "Cross Section Values to Use in Analyzing the Cesium Thermionic Converter," Thermionic Conversion Specialist Conference, Cleveland, Ohio, October 1964.

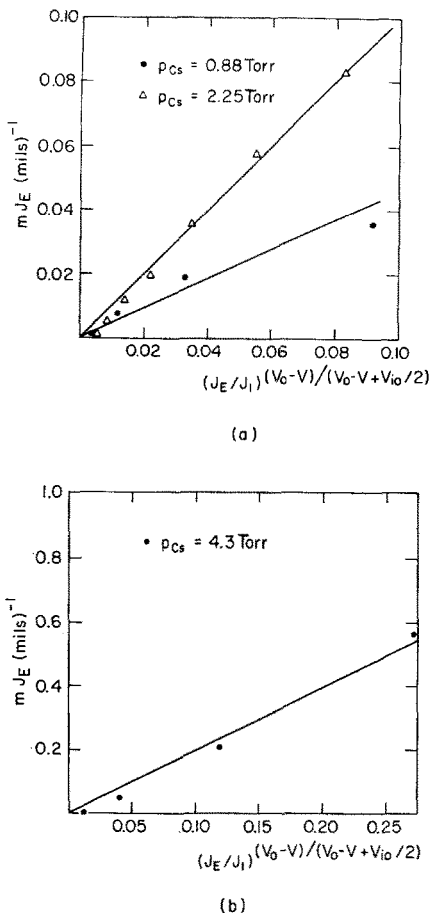


FIG. 5. Plots of  $mJ_E$  vs  $(J_E/J_1)(V_0-V)/(V_0-V+0.5V_{i0})$  used for the determination of  $D$ : (a)  $p_{Cs}=0.88$  and  $2.25$  Torr; (b)  $p_{Cs}=4.3$  Torr.

Note that for each cesium pressure the data behave as predicted by Eq. (19b). Values of  $J_E$  and  $\phi_E$  determined from these data are given in Table II. Although crude estimates of  $D$  may also be inferred from Fig. 4, it is better to use the procedure suggested by Eq. (21b) for this purpose.

Figure 5 presents plots of  $mJ_E$  vs

$$(J_E/J_1)(V_0-V)/(V_0-V+0.5V_{i0})$$

for the data shown in Fig. 4. In evaluating  $J_1$  it is assumed that  $T_{e0}=2500^\circ\text{K}$ ,  $\psi_e(T_{e0})=1$ , and  $C_2=5$ , recognizing the insensitivity of the results to these values. The values of the collector work function are taken from Ref. 1 and they are shown in Table II. Note that the data in Fig. 5 do indeed fall on straight lines as predicted by Eq. (19b). Values of  $D$  and  $\sigma_{en}/C_2$  determined from the slopes of these lines are given in Table II.

The derived emitter work functions are in good agreement ( $\pm 0.1$  eV) with values obtained in independent emission studies.<sup>11</sup> Also, the values obtained for the

<sup>11</sup> S. Kitrilakis (private communication).

TABLE II. Converter parameters determined from Figs. 5 and 6.

$p_{Cs}$ (Torr)	$J_E$ (A/cm <sup>2</sup> )	$\phi_E$ (eV)	$\phi_C$ (eV)	$V_0$ (eV)	$D$ (mil)	$\sigma_{en}/C_2$ (A <sup>2</sup> )
0.88	4.08	2.85	1.85	1.00	2.18	350
2.25	20.0	2.60	1.90	0.70	1.00	300
4.30	62.5	2.43	1.88	0.55	0.50	310

ratio  $\sigma_{en}/C_2$  are consistent with the values of  $\sigma_{en}$  and  $C_2$  obtained from the analysis of electron random current density profiles (see Sec. 4.2). It should be pointed out, however, that output-current characteristics do not provide adequate information for the individual determination of  $\sigma_{en}$  and  $C_2$ .

The comparison of individual theoretical and experimental output-current characteristics is shown in Fig. 6. The solid curves are the experimental variable spacing output-current characteristics reported in Ref. 1 for  $p_{Cs}=2.25$  Torr. The dashed curves are the theoretical predictions obtained using Eq. (19b) and the converter parameters listed in Table II for  $p_{Cs}=2.25$  Torr. Note that the theoretical and experimental output-current characteristics for  $d=16, 32,$  and  $64$  mils are in good agreement throughout the range of ignited mode vicinity of the transition into the extinguished mode of operation. This agreement is consistent with Ineq. (18) and indicates that, for these spacings, the thermionic converter does not enter an "obstructed" mode of operation<sup>1</sup> even though the emission is considerably electron rich under the conditions described in Fig. 6. For  $d=8$  mils ( $R_e \approx 10$ ) the theoretical analysis begins to break down at low currents. Whether this failure is due to the transition of the discharge into an obstructed mode or due to the inapplicability of the collisional, quasi-equilibrium analysis cannot be accurately stated. The conclusion to be drawn from these observations is that the obstructed mode is by no means an essential feature of thermionic converter output-current characteristics since a wide region of converter operation can be described without postulating its existence.

The insensitivity of the output-current characteristics

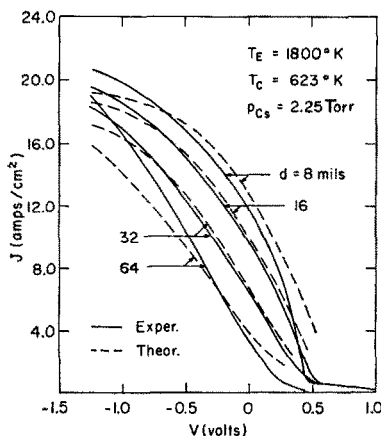
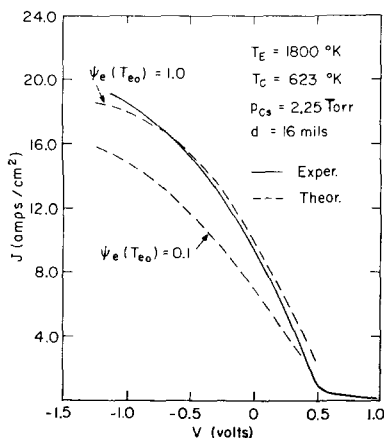


FIG. 6. Comparison of experimental<sup>1</sup> and theoretical output-current characteristics.

FIG. 7. Illustrative example of insensitivity of output-current characteristics to  $\psi_e(T_{e0})$ .



to the parameter  $\psi_e(T_{e0})$  which characterizes the volume ionization-recombination process is illustrated in Fig. 7. The solid curve is the experimental output-current characteristic of Fig. 6 for  $d=16$  mils. The dashed curves are the theoretical predictions obtained using Eq. (19b) for  $\psi_e(T_{e0})=1.0$  and  $\psi_e(T_{e0})=0.1$  and values of the other parameters as listed in Table II for  $p_{Cs}=2.25$  Torr. It is clear that an order of magnitude change in  $\psi_e(T_{e0})$  results in a small change in the output-current characteristics.

## 5. CONCLUSIONS

In low-energy plasmas with many collisions and in which the ionization-recombination mechanisms are of the multistage type, a state of quasi-equilibrium ex-

ists throughout most of the plasma provided that the electron temperature is a few hundred degrees higher than the ignition temperature. Serious conceptual errors may result if the recombination process is neglected.

The assumption of quasi-equilibrium in the inter-electrode plasma of a thermionic converter operating in the ignited mode leads to a plasma model which correlates a wide variety of experimental data. Included in the successful correlations are electron random current density and temperature profiles as well as output-current characteristics. The correlation constants are in satisfactory agreement with theoretical values and independent measurements.

The experimentally observed state of quasi-equilibrium in thermionic converter plasmas indicates that these plasmas are very nearly in a state of local Saha equilibrium throughout. This suggests that the ionization-recombination process is a multistage one involving numerous excited states and leading to the formation of atomic cesium ions.

Electron density profiles, as well as output-current characteristics, are extremely insensitive to the specific ionization-recombination processes, and consequently yield little information relating to these processes.

The ignited mode can be described without dividing it into obstructed and saturation modes.

## ACKNOWLEDGMENT

The first author gratefully acknowledges a fellowship granted by the Thompson-Ramo-Wooldridge Space Technology Laboratories.